

Switching on Supramolecular Catalysis via Cavity Mediation and Electrostatic Regulation

Yupu Qiao, Long Zhang,* Jia Li, Wei Lin,* and Zhenqiang Wang*

Abstract: Synthetic supercontainers constructed from divalent metal ions, carboxylate linkers, and sulfonylcalix[4]arene-based container precursors exhibit great promise as enzyme mimics that function in organic solvents. The capacity of these artificial hosts to catalyze Knoevenagel condensation can be switched on when the aldehyde substrate possesses a molecular size and shape matching the nanocavity of the supercontainers. In contrast, little reactivity is observed for other aldehydes that do not match the binding pocket. This substrate-dependent catalytic selectivity is attributed to the Brønsted acidity of the metal-bound water molecules located inside the nanocavity, which is amplified when the size/shape of the aldehyde substrate fits the binding cavity. The electrostatic environment of the binding cavity and the Brønsted acidity of the supercontainer can be further modulated using tetraalkylammonium-based regulators, leading to higher reactivity for the otherwise unreactive aldehydes.

Enzymes are Nature's catalysts par excellence. By virtue of their remarkable substrate selectivity, superior catalytic efficiency, and mild operational conditions, enzymes have provided the ultimate inspiration for researchers interested in catalyst design.^[1] Several critical elements, including precise organization of the substrate within the close proximity of the binding pocket and well-tuned electrostatic environment of the active site, are widely recognized as key to the ability of enzymes to accelerate otherwise sluggish chemical reactions in an astonishingly efficient manner.^[2] Chemists have long endeavored to emulate such elegant efficacy in synthetic catalytic systems, particularly through rational design of artificial constructs using supramolecular chemistry principles.^[3] Indeed, supramolecular catalysis by container mole-

cules has emerged as a promising approach to mimicking enzymatic catalysis.^[4] Container molecules are well suited for this task, as they possess chemically tunable nanocavity that can imitate the microenvironment of enzyme binding pockets and harness multiple non-covalent interactions in a synergistic manner.^[5] However, despite the impressive progress made in the last decades, designing enzyme-like, cavity-mediated supramolecular catalysis remains generally challenging, which is due in no small measure to the prevalence of product inhibition.^[6] Furthermore, the ability to regulate catalytic processes using small molecules or ions via an allosteric^[7] or electrostatic^[8] mechanism, a strategy masterfully employed by Nature to modulate enzyme functions, has been relatively elusive to attain in synthetic systems.^[9] Herein, we discuss how these critical issues can be addressed in a new class of synthetic supercontainers, wherein their ability to promote supramolecular catalysis can be switched on through selective recognition of the substrate size/shape and electrostatic modulation of the binding pocket via cationic regula-

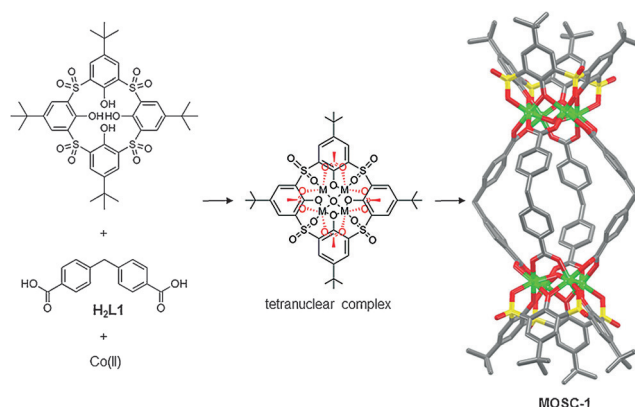
We recently reported a unique family of coordination containers, termed metal-organic supercontainers (MOSCs), which were obtained from the assembly of sulfonylcalix[4]arene-based container precursors,^[10] divalent metal ions, and carboxylate linkers of various shapes.^[11] For example, the reaction of *p*-tert-butylsulfonylcalix[4]arene (TBSC), Co^{II} or Ni^{II}, and an angular semi-flexible dicarboxylate linker such as 4,4'-methylenedibenzoic acid (H₂L1) or 4,4'-iminobis(methylene)-dibenzoic acid (H₂L2), gave rise to two members of the type IV MOSC family, designated here as MOSC-1 and MOSC-2, respectively (Scheme 1; Supporting Information, Scheme S1).^[11e] These type IV MOSCs possess both *endo* and *exo* cavities and thus exhibit the trademark multi-pore architecture also observed in other prototypes of MOSCs.

[*] Dr. Y. Qiao, Dr. J. Li, Prof. Dr. Z. Wang
Department of Chemistry, University of South Dakota
414 East Clark Street, Churchill-Haines Laboratories, Room 115
Vermillion, SD 57069-2390 (USA)
E-mail: Zhenqiang.Wang@usd.edu

Dr. L. Zhang
Beijing National Laboratory for Molecular Sciences
CAS Key Laboratory of Molecular Recognition and Function
Institute of Chemistry, Chinese Academy of Sciences
Beijing, 100190 (China)
E-mail: zhanglong@iccas.ac.cn

Dr. W. Lin
Department of Chemistry, University of Minnesota
Minneapolis, MN 55455 (USA)
E-mail: antifreeze@protein@gmail.com

Supporting information and the ORCID identification number(s) for the author(s) of this article can be found under:
<http://dx.doi.org/10.1002/anie.201606847>.



Scheme 1. Assembly of supercontainer MOSC-1.

The cylindrically-shaped type IV MOSCs can be described as consisting of four dicarboxylate linkers bridging two tetranuclear complexes,^[12] each of which contains four metal ions coordinating to one TBSC unit, four carboxylate groups, and one presumed μ_4 -H₂O species (Scheme 1; Supporting Information, Scheme S1).

Previous preliminary findings suggested that, owing to its Lewis basicity derived from its secondary amine group, MOSC-2 exhibited excellent catalytic activity for the Knoevenagel condensation^[13] involving the nucleophilic addition of malononitrile (**2a**) to 2-naphthaldehyde (**1b**).^[11e] This supramolecular reactivity was consistent with the generally accepted reaction mechanism, which typically involves an amine base promoting the formation of a β -hydroxy intermediate and/or an iminium intermediate.^[14] Follow-up studies revealed that MOSC-2 also effectively catalyzed the reaction for a range of other aldehydes (Table 1). Interestingly, there appeared to be no direct correlation between the reactivity and the aldehyde size, since bulkier 1-pyrenecarboxaldehyde (**1e**) and smaller 2-naphthaldehyde (**1b**) both gave a similar, near-quantitative yield (95% vs. 92%). In contrast, a shape

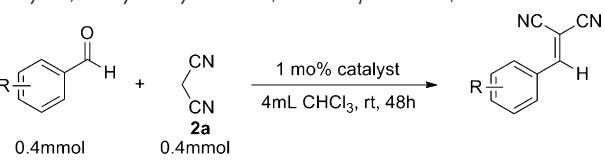
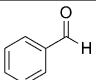
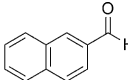
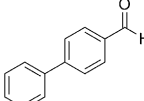
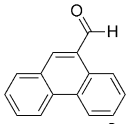
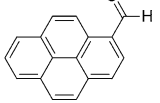
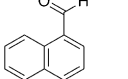
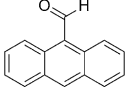
selectivity with regard to the aldehyde was clearly observed, as evidenced by the substantially lower yield of 1-naphthaldehyde (**1f**, 34%) than that of **1b** (92%) under otherwise identical conditions. A similarly moderate yield (44%) was also noted for 9-anthracenecarboxaldehyde (**1g**), a close structural analogue of **1f**. This interesting contrast of reactivity between the two groups of substrates, which orientate their aldehyde moiety in a manner that can be described as “parallel” and “perpendicular” to their aromatic backbone, respectively (Table 1, entries a–e vs. f and g; Supporting Information, Scheme S2), suggests that the aldehyde substrate binds to the MOSC in a spatially defined manner, likely driven by the cylindrical shape of the MOSC *endo* cavity dictating the specific host–guest binding geometry (see below).

To interrogate this intriguing trend of reactivity, we examined MOSC-1, a non-amine analogue of MOSC-2, and discovered that, not so surprisingly, it showed negligible catalytic activity towards the majority of the aldehydes examined above (Table 1), owing to its lack of Lewis basicity. Strikingly though, one particular substrate, namely **1e**, stood out as a notable exception. The Knoevenagel condensation of **1e** with **2a** was effectively catalyzed by MOSC-1, giving rise to a decent yield of 67% using 1 mol% loading of the supramolecular catalyst. While the base-promoted β -hydroxy or iminium intermediate constitutes the most common reaction mechanism, this unexpected result and unusual substrate selectivity prompted us to re-evaluate the underpinning of the MOSC-catalyzed reactions. Several previous reports suggested that a Brønsted acid can also facilitate the Knoevenagel condensation through protonation of the aldehyde group.^[15] Although acid-catalyzed Knoevenagel reactions are generally rare presumably as a result of the propensity of the acid catalyst to neutralize the deprotonated nucleophile, we reason that such an undesired quenching effect may be avoided if the Brønsted acid is properly immobilized in a porous matrix, as implied by the study of Saravanamurugan et al.^[15a]

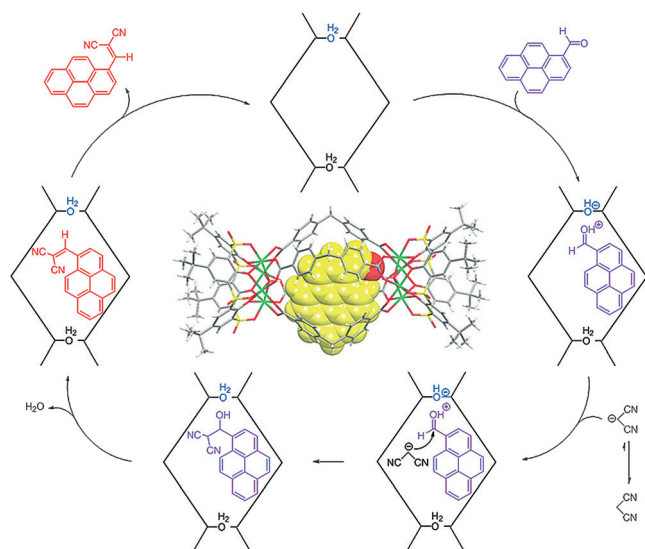
In light of this scenario, we propose the following reaction mechanism (Scheme 2) and attribute the catalytic activity of MOSC-1 towards **1e** to its Brønsted acidity originating from Co^{II}-bound μ_4 -H₂O. Specifically, the substrates (**1e** and **2a**) bind to the *endo* cavity of MOSC-1, and the μ_4 -H₂O located inside then protonates the carbonyl group of **1e**, activating the aldehyde substrate and enhancing its electrophilicity with **2a**. The so-formed β -hydroxy intermediate undergoes dehydration and gives rise to the final alkenyl product, which is released from the cavity owing to its relative bulkiness. The substrate selectivity with regard to **1e** can be rationalized on the basis of a lock-and-key type match between MOSC-1 and **1e**. The relatively weak Brønsted acidity of the μ_4 -H₂O means that MOSC-1 does not readily protonate and activate an aldehyde unless the substrate possesses a suitable molecular size and shape to fit inside the cavity and allow its aldehyde moiety to be pre-organized within the close proximity of the active site.

The proposed mechanism was supported by several lines of considerations. A particularly enlightening evidence came from our density functional theory (DFT) calculation, which

Table 1: Yields for Knoevenagel reactions of malononitrile with various aldehydes, catalyzed by MOSC-1, MOSC-1/TMA⁺Cl[−], and MOSC-2.^[a]

|  | | | | |
|--|---|--------|--|--------|
| Entry | Aldehyde | MOSC-1 | Yield [%] MOSC-1/ TMA ⁺ Cl [−] | MOSC-2 |
| a |  | 7 | 46 | 67 |
| b |  | 5 | 62 | 92 |
| c |  | 1 | 33 | 89 |
| d |  | 2 | 34 | 81 |
| e |  | 67 | 55 | 95 |
| f |  | 3 | 50 | 34 |
| g |  | 3 | 40 | 44 |

[a] TMA⁺ = Tetramethylammonium cation; 6 mol% of TMA⁺Cl[−] was used.



Scheme 2. Proposed mechanism for the Knoevenagel condensation catalyzed by MOSC-1.

indicated that **1e** was indeed capable of binding to the *endo* cavity of MOSC-1 and pre-aligning its carbonyl group near the active site (Supporting Information, Figure S4a). The substrate recognition was achieved partly through the μ_4 -H₂O molecule hydrogen-bonding with the carbonyl oxygen of **1e** (O \cdots O 2.73 Å). Multiple C–H \cdots π interactions were also abundantly present between the phenyl moieties of the MOSC *endo* cavity and the pyrene backbone of **1e**. These C–H \cdots π interactions, while individually weak,^[16] contributed in a concerted manner to organizing the substrate in its pre-reactive conformation. It is not difficult to envisage that similar synergistic C–H \cdots π interactions may have also been implicated in the MOSC-2 system and accounted for its shape selectivity discussed above. Specifically, the carbonyl groups of the perpendicular aldehydes were likely forced to point away from the μ_4 -H₂O center as a result of the preferred orientation of the C–H \cdots π interactions, rendering these aldehydes less effectively activated. Additional DFT calculation revealed that the O–H bond lengths of the μ_4 -H₂O species were slightly longer than that of a free H₂O molecule by up to 0.086 Å (Supporting Information, Figure S4b), consistent with its proposed weak but substantial Brønsted acidity.

A second experiment comparing the reactivity of malononitrile (**2a**) with that of Meldrum's acid (**2b**) provided additional mechanistic insights. **2b** is known to be more acidic than **2a** ($pK_a = 7.3$ vs. 11.1 in DMSO)^[17] and thus represents a generally better nucleophile than the latter. This was evidenced by its higher reactivity with **1e** (by more than twice) when Me₂L2, the dimethyl ester of H₂L2, was used as a small-molecule catalyst (Supporting Information, Table S4). However, replacing Me₂L2 with the supramolecular catalyst MOSC-1 led to nearly 80% decrease for **2b** but a more than threefold increase for **2a** in their respective reaction yield, making **2b** a significantly less effective nucleophile and reversing the relative trend of reactivity. This interesting finding is in line with the proposal that the Knoevenagel

reaction takes place inside the MOSC *endo* cavity, as the impeded reactivity of **2b** in the presence of MOSC-1 can be attributed to its higher steric bulk within the restricted nanoenvironment of the *endo* cavity.

The most profound implication of the proposed mechanism was the realization that the catalytic efficacy of MOSC-1 could be regulated by cations serving as electrostatic effectors. A conceivable rationale was that a suitable cation may enhance the Brønsted acidity of the μ_4 -H₂O through stabilizing the deprotonated OH[−] anion. This reasoning was indeed experimentally confirmed by adding the chloride salt of tetramethylammonium (TMA⁺) cation to the MOSC-1 promoted reactions involving **2a** and various aldehydes. In the presence of TMA⁺, the otherwise unreactive aldehydes examined above exhibited a substantially higher reactivity and readily underwent the Knoevenagel reaction (Table 1). Interestingly, unlike these smaller aldehydes, **1e** actually showed a slightly lower yield with TMA⁺ than without it (55% vs. 67%). Close examination of the reaction kinetics nevertheless revealed that the combination of MOSC-1 and TMA⁺ did significantly enhance the reaction rate of **1e** in the initial stage of the reaction (Figure 1). Without TMA⁺, the

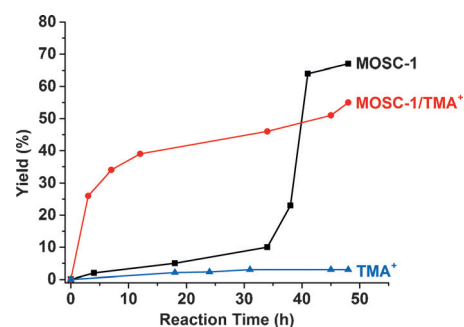


Figure 1. Reaction kinetics of the Knoevenagel condensation of 1-pyrenecarboxaldehyde with malononitrile, in the presence of MOSC-1 (black), MOSC-1/TMA⁺ (red), and TMA⁺ (blue), respectively.

reaction consisted of an induction period, in which little product was formed in the first 35 hours. The product generation rapidly accelerated after this period, quickly reaching saturation within about 5 hours. In contrast, the addition of TMA⁺ (6 equiv to MOSC-1) to the reaction mixture eliminated the induction period and the product formation became apparent almost immediately. It is worth noting that TMA⁺ alone did not catalyze the Knoevenagel reaction. This thus suggests that to promote the reaction, TMA⁺ must partner with MOSC-1, most likely through binding to the MOSC *endo* cavity via electrostatic interactions.^[18] The importance of the *endo* cavity on the catalysis was further illustrated by the lack of Knoevenagel reactivity observed for **1e** when MOSC-1 was substituted by a tetranuclear complex (with or without TMA⁺; Supporting Information, Table S5), which has an *exo* cavity nearly identical to that of MOSC-1 but possesses no *endo* cavity.

The small amount of reduction of the overall yield for **1e** in the presence of TMA⁺ can be attributed to the cation competing with the substrates for the limited nanospace of the

MOSC *endo* cavity. Such a steric effect was even more evident when TMA⁺ was replaced by a series of related cationic regulators, such as tetraethylammonium (TEA⁺), tetrapropylammonium (TPA⁺), and tetrabutylammonium (TBA⁺). The increasingly larger size of the cations led to growing sterics that effectively cancelled out the positive electrostatic effect and resulted in a gradual decrease of the reaction yield (Supporting Information, Figure S5). As indicated above, a similar steric effect was also implicated in the MOSC-catalyzed reaction involving **2b**.

To further pinpoint how the tetraalkylammonium cations interacted with the MOSC, we obtained MOSC-1', an isomeric structure to MOSC-1, by replacing Co^{II} with Zn^{II} in the synthesis (see the Supporting Information). The diamagnetic nature of MOSC-1' allowed us to use the NMR spectroscopy to probe the ammonium binding of the MOSC in CDCl₃. In the absence of a guest, the ¹H NMR spectrum of MOSC-1' featured broad and poorly separated peaks (Supporting Information, Figure S6), which we attributed to the MOSC molecules aggregating in the solution. While adding the aldehydes or **2a** did not improve the spectrum, the addition of an excess amount of TBA⁺ to the solution led to a drastically simpler spectrum with well-defined peaks (Figure 2). The protons of one equivalent of TBA⁺ underwent

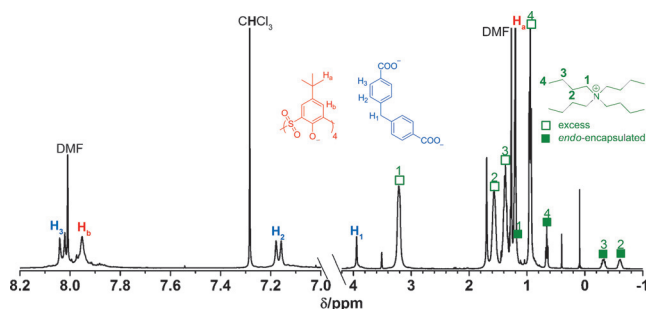


Figure 2. ¹H NMR spectrum of TBA⁺@MOSC-1' in CDCl₃. The molar ratio of TBA⁺:MOSC-1' is ca. 6.

a significant upfield shift, indicating its encapsulation inside the *endo* cavity. The much larger up-field shift of α -protons ($\Delta\delta \approx 2.02$ ppm), compared with that of δ -protons ($\Delta\delta \approx 0.26$ ppm), suggested that the positive charge of TBA⁺ was located deeper inside the binding pocket than its alkyl ends, consistent with the proposed electrostatic mechanism. The 1:1 binding ratio was verified by the Job's plot based on a UV/Vis study of MOSC-1 (Supporting Information, Figure S7). The *endo*-capsulation of TBA⁺ by the MOSC was unambiguously confirmed by a ¹H-¹H nuclear Overhauser effect spectroscopy (NOESY) experiment (Supporting Information, Figure S8). While the excess TBA⁺ did not show any noticeable up-field shift, the NOESY spectrum revealed its binding to the *exo* cavities.^[19] Replacing TBA⁺ with TPA⁺, TEA⁺, or TMA⁺ similarly improved the ¹H NMR spectrum of MOSC-1', although it exhibited a strong dependency on the cation size, as the smaller TEA⁺ and TMA⁺ gave rise to a more complex NMR pattern, which is presumably due to

their faster motion in and out of the *endo* cavity (Supporting Information, Figures S9–S11).^[20]

The validation of molecular recognition occurring at both the *endo* and *exo* sites underscored the exciting potentials afforded by the trademark multi-pore architecture of the MOSCs, and begged the intriguing question of whether the *exo* binding event also contributed to regulating the catalysis. Comparing the kinetic profiles of the reactions involving **1e**, **2a**, MOSC-1, and 0–9 equivalents of TMA⁺ indicated that the reactivity was strongly influenced by the amount of TMA⁺ added (Supporting Information, Figure S12). Since there is only one equivalent of TMA⁺ residing inside the *endo* cavity, and additional TMA⁺ equivalents must be located outside the substrate binding pocket, this finding suggested that the MOSC-based catalyst system likely employed an unconventional allosteric mechanism, in which electrostatic interactions, instead of, or in addition to, conformational changes, were used to regulate the catalysis.^[7a,21]

In short, we successfully utilized a new class of container molecules to harvest several trademark features of enzymatic catalysis. We made use of two particularly important elements, namely selective substrate recognition and electrostatic/allosteric regulation, to switch on supramolecular catalysis. The ability to demonstrate such biomimetic characteristics in synthetic and non-aqueous systems has profound implications for designing highly functional, complex, and modular enzyme mimics. In particular, the viability to employ task-specific small-molecule regulators to modulate chemical reactions is anticipated to afford unprecedented opportunities in asymmetric catalysis, photocatalysis, and other related areas.

Acknowledgements

This research was supported by a National Science Foundation CAREER Award CHE-1352279. Z.W., Y.Q., and J.L. also acknowledge an NSF MRI Award CHE-1229035 for the purchase of a Bruker 400 MHz NMR spectrometer.

Keywords: calixarenes · container molecules · Knoevenagel condensation · supramolecular catalysis · tetraalkylammonium

How to cite: *Angew. Chem. Int. Ed.* **2016**, *55*, 12778–12782
Angew. Chem. **2016**, *128*, 12970–12974

- [1] a) C.-H. Wong, G. M. Whitesides, *Enzymes in synthetic organic chemistry*, 1st ed., Pergamon, Elsevier Science Oxford, UK, Tarrytown, N.Y., **1994**; b) K. Drauz, H. Gröger, O. May, *Enzyme catalysis in organic synthesis: a comprehensive handbook*, 3rd ed., Wiley-VCH, Weinheim, **2012**; c) A. M. Klibanov, *Nature* **2001**, *409*, 241–246.
- [2] D. Ringe, G. A. Petsko, *Science* **2008**, *320*, 1428–1429.
- [3] J. M. Lehn, *Supramolecular Chemistry*, Wiley, New York, **1995**.
- [4] a) F. Cramer, W. Kampe, *J. Am. Chem. Soc.* **1965**, *87*, 1115–1120; b) R. Breslow, S. D. Dong, *Chem. Rev.* **1998**, *98*, 1997–2011; c) J. M. Kang, J. Santamaria, G. Hilmersson, J. Rebek, *J. Am. Chem. Soc.* **1998**, *120*, 7389–7390; d) M. Yoshizawa, M. Tamura, M. Fujita, *Science* **2006**, *312*, 251–254; e) M. D. Pluth, R. G. Bergman, K. N. Raymond, *Science* **2007**, *316*, 85–88;

- f) D. M. Kaphan, M. D. Levin, R. G. Bergman, K. N. Raymond, F. D. Toste, *Science* **2015**, *350*, 1235–1238; g) C. J. Brown, F. D. Toste, R. G. Bergman, K. N. Raymond, *Chem. Rev.* **2015**, *115*, 3012–3035; h) M. L. Merlau, M. D. P. Mejia, S. T. Nguyen, J. T. Hupp, *Angew. Chem. Int. Ed.* **2001**, *40*, 4239–4242; *Angew. Chem.* **2001**, *113*, 4369–4372; i) J. Meeuwissen, J. N. Reek, *Nat. Chem.* **2010**, *2*, 615–621; j) Q. Zhang, K. Tiefenbacher, *Nat. Chem.* **2015**, *7*, 197–202; k) W. Cullen, M. C. Misuraca, C. A. Hunter, N. H. Williams, M. D. Ward, *Nat. Chem.* **2016**, *8*, 231–236; l) Q.-Q. Wang, S. Gonell, S. H. A. M. Leenders, M. Dürr, I. Ivanović-Burmazović, J. N. H. Reek, *Nat. Chem.* **2016**, *8*, 225–230.
- [5] D. J. Cram, J. M. Cram, *Container Molecules and Their Guests*, The Royal Society of Chemistry, Cambridge, **1997**.
- [6] a) J. M. Kang, J. Rebek, *Nature* **1997**, *385*, 50–52; b) R. J. Hooley, *Nat. Chem.* **2016**, *8*, 202–204.
- [7] a) N. M. Goodey, S. J. Benkovic, *Nat. Chem. Biol.* **2008**, *4*, 474–482; b) C. J. Tsai, A. del Sol, R. Nussinov, *J. Mol. Biol.* **2008**, *378*, 1–11.
- [8] A. Warshel, P. K. Sharma, M. Kato, Y. Xiang, H. Liu, M. H. Olsson, *Chem. Rev.* **2006**, *106*, 3210–3235.
- [9] a) J.-L. Pierre, G. Gagnaire, P. Chautemps, *Tetrahedron Lett.* **1992**, *33*, 217–220; b) I. O. Fritsky, R. Ott, R. Krämer, *Angew. Chem. Int. Ed.* **2000**, *39*, 3255–3258; *Angew. Chem.* **2000**, *112*, 3403–3406; c) L. Kovbasyuk, R. Krämer, *Chem. Rev.* **2004**, *104*, 3161–3187; d) N. C. Gianneschi, P. A. Bertin, S. T. Nguyen, C. A. Mirkin, L. N. Zakharov, A. L. Rheingold, *J. Am. Chem. Soc.* **2003**, *125*, 10508–10509; e) N. C. Gianneschi, S. T. Nguyen, C. A. Mirkin, *J. Am. Chem. Soc.* **2005**, *127*, 1644–1645; f) N. C. Gianneschi, M. S. Masar, C. A. Mirkin, *Acc. Chem. Res.* **2005**, *38*, 825–837; g) H. J. Yoon, J. Kuwabara, J. H. Kim, C. A. Mirkin, *Science* **2010**, *330*, 66–69; h) A. Scarso, G. Zaupa, F. B. Houillon, L. J. Prins, P. Scrimin, *J. Org. Chem.* **2007**, *72*, 376–385; i) S. Ghosh, L. Isaacs, *J. Am. Chem. Soc.* **2010**, *132*, 4445–4454; j) C. Kremer, A. Lutzen, *Chem. Eur. J.* **2013**, *19*, 6162–6196; k) M. Raynal, P. Ballester, A. Vidal-Ferran, P. W. van Leeuwen, *Chem. Soc. Rev.* **2014**, *43*, 1734–1787.
- [10] a) N. Iki, H. Kumagai, N. Morohashi, K. Ejima, M. Hasegawa, S. Miyanari, S. Miyano, *Tetrahedron Lett.* **1998**, *39*, 7559–7562; b) N. Morohashi, F. Narumi, N. Iki, T. Hattori, S. Miyano, *Chem. Rev.* **2006**, *106*, 5291–5316.
- [11] a) F.-R. Dai, Z. Wang, *J. Am. Chem. Soc.* **2012**, *134*, 8002–8005; b) F.-R. Dai, U. Sambasivam, A. J. Hammerstrom, Z. Wang, *J. Am. Chem. Soc.* **2014**, *136*, 7480–7491; c) N. L. Netzer, F.-R. Dai, Z. Wang, C. Jiang, *Angew. Chem. Int. Ed.* **2014**, *53*, 10965–10969; *Angew. Chem.* **2014**, *126*, 11145–11149; d) F.-R. Dai, D. C. Becht, Z. Wang, *Chem. Commun.* **2014**, *50*, 5385–5387; e) F.-R. Dai, Y. Qiao, Z. Wang, *Inorg. Chem. Front.* **2016**, *3*, 243–249.
- [12] T. Kajiwarra, T. Kobashi, R. Shinagawa, T. Ito, S. Takaishi, M. Yamashita, N. Iki, *Eur. J. Inorg. Chem.* **2006**, 1765–1770.
- [13] E. Knoevenagel, *Ber. Dtsch. Chem. Ges.* **1898**, *31*, 2596–2619.
- [14] a) O. B. Berryman, A. C. Sather, A. Lledo, J. Rebek, Jr., *Angew. Chem. Int. Ed.* **2011**, *50*, 9400–9403; *Angew. Chem.* **2011**, *123*, 9572–9575; b) T. Murase, Y. Nishijima, M. Fujita, *J. Am. Chem. Soc.* **2012**, *134*, 162–164; c) D. Samanta, S. Mukherjee, Y. P. Patil, P. S. Mukherjee, *Chem. Eur. J.* **2012**, *18*, 12322–12329.
- [15] a) S. Saravanamurugan, M. Palanichamy, M. Hartmann, V. Murugesan, *Appl. Catal. A* **2006**, *298*, 8–15; b) G. Thirupathi, M. Venkatanarayana, P. Dubey, Y. Bharathi Kumari, *Der. Pharma. Chemica* **2012**, *14*, 1897–1901.
- [16] M. Nishio, *Phys. Chem. Chem. Phys.* **2011**, *13*, 13873–13900.
- [17] a) E. M. Arnett, S. G. Maroldo, S. L. Schilling, J. A. Harrelson, *J. Am. Chem. Soc.* **1984**, *106*, 6759–6767; b) W. S. Matthews, J. E. Bares, J. E. Bartmess, F. G. Bordwell, F. J. Cornforth, G. E. Drucker, Z. Margolin, R. J. McCallum, G. J. McCollum, N. R. Vanier, *J. Am. Chem. Soc.* **1975**, *97*, 7006–7014.
- [18] a) M. T. Reetz, S. Huette, R. Goddard, *J. Am. Chem. Soc.* **1993**, *115*, 9339–9340; b) S. Shirakawa, S. Liu, S. Kaneko, Y. Kumatabara, A. Fukuda, Y. Omagari, K. Maruoka, *Angew. Chem. Int. Ed.* **2015**, *54*, 15767–15770; *Angew. Chem.* **2015**, *127*, 15993–15996.
- [19] It appears that some of the excess TBA⁺ may also bind to the outside wall of the *endo* cavity.
- [20] D. L. Caulder, R. E. Powers, T. N. Parac, K. N. Raymond, *Angew. Chem. Int. Ed.* **1998**, *37*, 1840–1843; *Angew. Chem.* **1998**, *110*, 1940–1943.
- [21] P. Hanoian, C. T. Liu, S. Hammes-Schiffer, S. Benkovic, *Acc. Chem. Res.* **2015**, *48*, 482–489.

Received: July 14, 2016

Revised: August 8, 2016

Published online: September 16, 2016